ELSEVIER

Biophysical Chemistry 92 (2001) 1–15

Biophysical Chemistry

www.elsevier.com/locate/bpc

A stochastic, molecular model of the fission yeast cell cycle: role of the nucleocytoplasmic ratio in cycle time regulation

Akos Sveiczer[a,*], John J. Tyson[b], Bela Novak[a]

[a] *Department of Agricultural Chemical Technology, Budapest University of Technology and Economics, 1521 Budapest, Szt. Gellert ter 4, Hungary*

[b] *Department of Biology, Virginia Polytechnic Institute and State University, Blacksburg, VA 24061, USA*

Received 18 January 2001; received in revised form 11 May 2001; accepted 29 May 2001

Abstract

We propose a stochastic version of a recently published, deterministic model of the molecular mechanism regulating the mitotic cell cycle of fission yeast, *Schizosaccharomyces pombe*. Stochasticity is introduced in two ways: (i) by considering the known asymmetry of cell division, which produces daughter cells of slightly different sizes; and (ii) by assuming that the nuclear volumes of the two newborn cells may also differ. In this model, the accumulation of cyclins in the nucleus is proportional to the ratio of cytoplasmic to nuclear volumes. We have simulated the cell-cycle statistics of populations of wild-type cells and of *wee1*$^-$ mutant cells. Our results are consistent with well known experimental observations.

Keywords: Cell cycle; Fission yeast; Stochastic model; Computational simulation; Size control; Nucleocytoplasmic ratio

1. Introduction

The cell division cycle is the sequence of events whereby a cell duplicates its components and divides them between two daughter cells, so that each daughter receives the information and machinery necessary to repeat the process. During a division cycle, the cell must execute the crucial events of chromosome replication and segregation in the correct order (DNA synthesis, followed by mitosis, followed by cytokinesis), and it must ensure that the chromosome replication cycle is synchronized to the mass-doubling cycle.

* Corresponding author. Tel.: +36-1-463-2349; fax: +36-1-463-2598.

E-mail address: sveiczer.mkt@chem.bme.hu (A. Sveiczer).

0301-4622/01/$ - see front matter
PII: S0301-4622(01)00183-1

The proper coordination of cell cycle events is enforced at so-called 'checkpoints', where progress through the chromosome cycle is halted until certain conditions are met, for example, completion of a prior event, or attainment of a critical cell size [1].

Intensive studies of the physiology of cell division started in the 1950s, and 20 years later genetic methods were introduced for isolating cell cycle mutants of both budding and fission yeasts. By the end of the 1980s, biochemists and molecular geneticists had identified the central molecular components of the cell-cycle control system, and many new genes and proteins have become known since then [2]. The simple unicellular eukaryote, *Schizosaccharomyces pombe* (fission yeast) has been an attractive model organism in all chapters of cell cycle research, since it is easy to handle by genetic, biochemical, and microscopic methods [3].

Early attempts to describe cell cycle regulation in mathematical terms were highly speculative, because reliable molecular descriptions of the control system were lacking before 1990, when the role of cyclin-dependent kinases in the chromosome replication cycle became clear [4]. Nonetheless, some interesting and influential theoretical studies appeared in the 1970s and 1980s: both deterministic models [5,6] and stochastic models [7–10]. With regard to fission yeast in particular, Alt and Tyson [11,12] proposed a stochastic model based on the nuclear accumulation of a hypothetical mitotic activator, in order to account for observed distributions of cycle times and division lengths in steady-state populations of wild-type cells. Later, Sveiczer and Novak [13] generated computer-simulated populations of Alt–Tyson 'cells' and showed that the properties of these simulated cells compared favorably with their own experimental observations of fission yeast cultures [14].

The explosion of molecular details about cyclin-dependent kinases and their partners in the early 1990s made possible the construction of more realistic mathematical models of the cell cycle [15–17]. In these molecular models, biochemical reactions were translated into systems of non-linear, ordinary differential equations (ODEs). By numerical simulation, the solution of these ODEs could be compared to the physiological behavior of living cells. This approach was used successfully to model the cell cycles of frog embryos [18,19], sea urchin embryos [20], budding yeast cells [21] and fission yeast cells [22–24]. Not only could these models explain the physiology of dividing cells in terms of the underlying molecular control system, but also they were able to account for the phenotypes of many classical cell-cycle mutants and to predict the behavior of yet unknown mutants. A disadvantage of deterministic ODE models is that they describe the behavior of a non-existing 'average cell', neglecting the differences among cells in culture.

The aim of the present study is to introduce stochastic element(s) into an ODE model of the molecular mechanism controlling the fission yeast cell cycle, to derive the distributions of cycle time and division size in a cell population, and to compare these distributions to observations of steady-state cultures of wild-type cells and *wee1*$^-$ mutants.

2. Model construction and simulations

2.1. The deterministic model

The underlying molecular network (Fig. 1) of the present model is a slightly modified version of our recently published model [25]. In the following description of the molecular mechanism, we refer to individual steps, as shown in Fig. 1. The fission yeast cell cycle is driven by fluctuations in the activity of M-phase promoting factor (MPF or Cdc13/Cdc2; shown in the middle of Fig. 1), which is a heterodimer of a catalytic subunit (Cdc2 protein kinase) and a regulatory subunit (the B-type cyclin Cdc13). The proper execution of cell cycle events requires that MPF activity oscillates between low (G1 phase), intermediate (S and G2 phases) and high (M phase) levels [26]. These different MPF levels are achieved by antagonistic relationships between MPF and its negative regulators: anaphase promoting complex (APC), Rum1 and Wee1/Mik1.

In the G1 phase, MPF activity is low for two

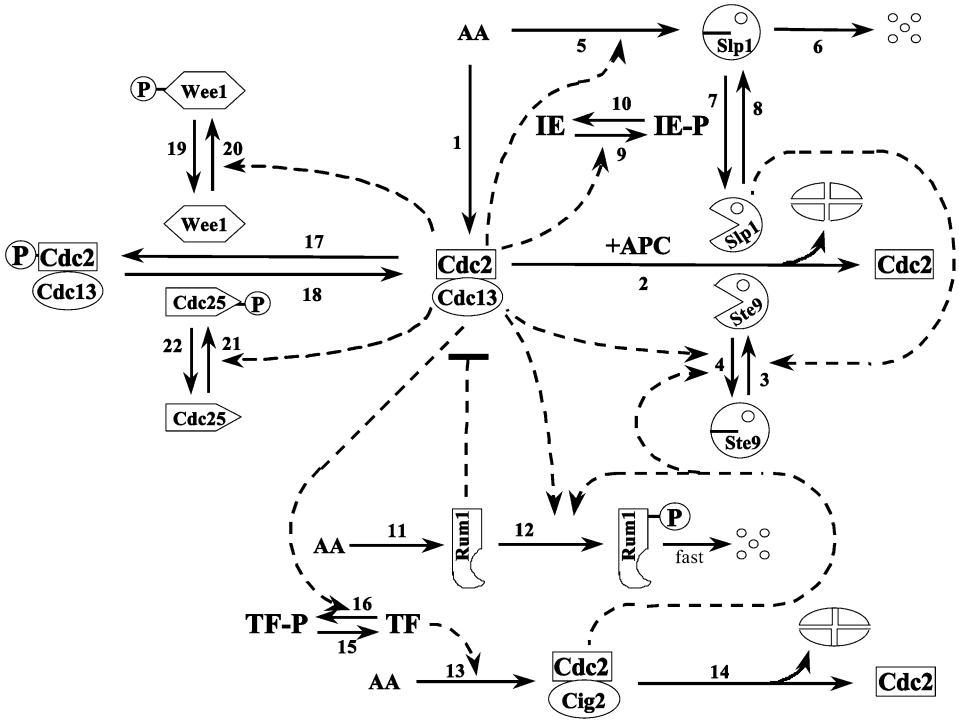

Fig. 1. A molecular mechanism for the regulation of Cdc13-associated kinase activity in fission yeast. All events of the fission yeast cell cycle can be orchestrated by fluctuations of the activity of a single cyclin-dependent kinase, Cdc13/Cdc2. Cdc13 is synthesized from amino acids (AA) and combines readily with catalytic subunits, Cdc2, which are assumed to be always present in excess. The activity of Cdc13/Cdc2 is modulated by Rum1 inhibition, by Tyr15-phosphorylation (via Wee1, which is reversed by Cdc25), and by Slp1/APC and Ste9/APC-dependent cyclin degradation. Other cyclins (Puc1, Cig1 and Cig2) in complex with Cdc2 can assist these processes.

reasons. First, Ste9 targets the Cdc13 subunit for ubiquitination by the APC (step 2 in Fig. 1) [27,28], and ultimately for degradation by proteasomes. Secondly, G1 cells contain abundant Rum1, a protein that binds to MPF and inhibits its activity (shown by a dashed line on Fig. 1) [29,30]. At the G1/S transition, both Ste9 [27,28] and Rum1 [31] are phosphorylated by MPF (steps 4 and 12, respectively), which inactivates the former and promotes the degradation of the latter (the phosphorylated form of Rum1 is assumed to degrade very fast). As a consequence, MPF activity starts to increase, cells pass the Start transition and commence DNA replication (S phase of the cell cycle). However, Cdc13/Cdc2 kinase is not fully activated at this time, because the Tyr-15 residue of Cdc2 is phosphorylated by two tyrosine kinases, Wee1 [32] and Mik1 [33] (step 17, Mik1 is not shown). Since this phosphorylation is inhibitory, MPF activity can reach only intermediate level (S and G2 phase of the cell cycle).[1] In the late G2 phase, this inhibitory phosphate group on Tyr-15 is removed by two tyrosine phosphatases, Cdc25 [34] and Pyp3 [35] (step 18, Pyp3 is not shown). MPF gets fully activated and this high MPF level drives the cell into mitosis (M phase). MPF activation at the G2/M boundary is characterized by positive feedback loops, since MPF phosphorylates both Wee1 (step 20; this is

[1] Both S and G2 phases are characterized by intermediate Cdc13/Cdc2 kinase activity; the only difference between them is whether DNA replication is ongoing or not.

inhibitory) and Cdc25 (step 21; this is activatory), and thereby stimulates its own activation [36].

At the end of mitosis, MPF activity must be eliminated to allow the cell to go back to G1 phase of the cycle. Exit from mitosis is induced by a negative feedback loop: MPF indirectly activates Slp1 (step 7) [37], which inactivates MPF. Slp1 (like Ste9) targets Cdc13 to the APC core, which causes Cdc13 ubiquitination and degradation (step 2). Similarly to Ste9, Slp1 is also regulated by MPF dependent phosphorylation. However, in contrast to Ste9, MPF mediated phosphorylation activates Slp1 rather than inactivates it. To create a time delay in the negative feedback, we put an intermediary enzyme (IE) between MPF and Slp1/APC that is reversibly phosphorylated (steps 9 and 10) [18]. By reducing MPF activity, Slp1 helps the reappearance of the two G1 regulators (Ste9 and Rum1), which have been kept inactive (Ste9) or at low level (Rum1) by MPF. We assume that Slp1 helps activate Ste9 through an additional mechanism (step 3), which could perhaps be mediated through a phosphatase (analogous to the Cdc14 protein of budding yeast). In summary, during the fission yeast cell cycle, Cdc13/Cdc2 kinase is regulated through antagonistic interactions with its enemies: Ste9, Rum1 and Wee1.

Wild-type fission yeast cells contain other cyclins (Puc1, Cig1 and Cig2), which also form complexes with Cdc2 [38]. These different cyclin/Cdc2 complexes help MPF (Cdc13/Cdc2) to phosphorylate and inactivate its enemies. They can do so, because they are less sensitive than MPF to Rum1 inhibition and APC-dependent degradation. Since the regulation of these cyclin/Cdc2 complexes is poorly understood in fission yeast, we choose only the most important complex, Cig2/Cdc2, as a dynamical variable in the model. Cig2 synthesis is mediated by a transcription factor (TF; step 13), which is a complex consisting of the product of the *cdc10* gene and other proteins. We assume that TF is activated in the nucleus in a cell mass-dependent manner by other cyclin/Cdk dimers (step 15), which can be either Puc1/Cdc2 [39] or Pas1/Pef1 kinase [40] or both (k_{15} in Table 1 corresponds to the effect of these kinases, which are not shown in Fig. 1). Once TF is activated, it promotes the synthesis of Cig2 (step 13), which complexes with Cdc2 to phosphorylate both Rum1 and Ste9 (steps 12 and 4, respectively). In this way, Cig2/Cdc2 helps MPF activity to appear and the cell to pass the G1/S transition. In addition, there is a negative feedback loop in G1/S control, because rising MPF activity inactivates the TF responsible for Cig2 synthesis.

This simple picture of Cig2 regulation is clearly incomplete. Although Cig2 is resistant to Ste9/APC [27,28], Rum1 can bind to and inhibit the Cig2/Cdc2 complex, but less efficiently than it does with Cdc13/Cdc2 [29,41]. In the present model, we ignore this inhibitory effect of Rum1 on Cig2/Cdc2.

The mechanism in Fig. 1 is converted into a set of ODEs (Table 1) by using standard principles of biochemical kinetics. We write a differential equation for the concentration of every component, where synthesis and activation increase the concentration (positive sign), whereas degradation and inactivation decrease it (negative sign). We assume that certain dynamic variables are in pseudo-steady state, which allows us to substitute algebraic equations for some ODEs [25]. After specifying the numerical values of numerous rate constants and Michaelis constants in these equations, we solve the dynamical system numerically to determine the concentrations of all variables as functions of time. Numerical values of these parameters (Table 1) were chosen so that the concentration profiles of cell cycle regulators are consistent with experiments on wild type (WT) and *wee1*$^-$ mutant cells.

A numerical simulation of the model with the parameter values in Table 1 yields the steady-state behavior of an average WT cell, if we ignore stochastic fluctuations in birth size (division asymmetry) and nuclear volume (Fig. 2a). The average cell is born at a relative size of 1, grows exponentially in time, and at size 2, it divides symmetrically into two identical daughter cells. During the short ($\sim$ 20 min) G1 phase [43], Ste9 keeps MPF activity low, by actively degrading Cdc13. However, there is no time for Rum1 to accumulate because TF is rapidly activated, producing Cig2-dependent kinase activity, which keeps Rum1 unstable and inactivates Ste9. Con-

Table 1
A mathematical model of the proposed mechanism (Fig. 1) for the fission yeast cell cycle

Differential equations[a]

$$\frac{d}{dt}Cdc13_T = k_1\text{-}k_2 \cdot Cdc13_T \qquad \frac{d}{dt}preMPF = k_{17} \cdot (Cdc13_T\text{-}preMPF)\text{-}k_{18} \cdot preMPF\text{-}k_2 \cdot preMPF$$

$$\frac{d}{dt}Ste9 = (k'_3 + k''_3 \cdot Slp1) \cdot \frac{1\text{-}Ste9}{J_3 + 1\text{-}Ste9}\text{-}(k_4 \cdot MPF + k'_4 \cdot Cig2) \cdot \frac{Ste9}{J_4 + Ste9} \qquad \frac{d}{dt}Slp1_T = k'_5 + k''_5 \cdot \frac{MPF^4}{J_5^4 + MPF^4}\text{-}k_6 \cdot Slp1_T$$

$$\frac{d}{dt}Slp1 = k_7 \cdot IE \cdot \frac{Slp1_T\text{-}Slp1}{J_7 + Slp1_T\text{-}Slp1}\text{-}k_8 \cdot \frac{Slp1}{J_8 + Slp1}\text{-}k_6 \cdot Slp1 \qquad \frac{d}{dt}IE = k_9 \cdot MPF \cdot \frac{1\text{-}IE}{J_9 + 1\text{-}IE}\text{-}k_{10} \cdot \frac{IE}{J_{10}\text{-}IE}$$

$$\frac{d}{dt}Rum1_T = k_{11}\text{-}k_{12} \cdot Rum1_T \qquad \frac{d}{dt}Cig2 = k_{13} \cdot TF\text{-}k_{14} \cdot Cig2 \qquad \frac{d}{dt}mass = \gamma \cdot mass$$

Further equations[b]

$$BB = Cdc13_T + Rum1_T + k_D \qquad Trimer = \frac{2 \cdot Cdc13_T \cdot Rum1_T}{BB + \sqrt{BB^2\text{-}4 \cdot Cdc13_T \cdot Rum1_T}}$$

$$\mathrm{MPF} = \frac{(Cdc13\text{T-}preMPF) \cdot (Cdc13\text{T-}Trimer)}{Cdc13\text{T}} \cdot \frac{mass}{NV}$$

$$TF = G(k_{15} \cdot mass/NV,\ k'_{16} + k''_{16} \cdot MPF,\ J_{15},\ J_{16}) \qquad Wee1 = G(V_{19},\ V_{20} \cdot MPF,\ J_{19},\ J_{20}) \qquad Cdc25 = G(V_{21} \cdot MPF,\ V_{22},\ J_{21},\ J_{22})$$

Rate functions

$$k_2 = V'_2 + V''_2 \cdot Ste9 + V'''_2 \cdot Slp1,\ k_{17} = V_{17} \cdot Wee1 + V'_{17},\ k_{18} = V_{18} \cdot Cdc25 + V'_{18},\ k_{12} = V'_{12} + V'''_{12} \cdot MPF + V''''_{12} \cdot Cig2$$

Switch

When MPF crosses 0.1 *from above, the cell divides functionally* ($mass \rightarrow mass \cdot DA$), *although cytokinesis happens much later in fission yeast*.

Rate constants (*for wild-type cells, all have dimensions* min^{-1})

$k_1 = 0.025$, $k'_3 = 1$, $k''_3 = 10$, $k_4 = 35$, $k'_4 = 2$, $k'_5 = 0.005$, $k''_5 = 0.2$, $k_6 = 0.1$, $k_7 = 1$, $k_8 = 0.5$, $k_9 = 0.1$, $k_{10} = 0.02$, $k_{11} = 1$, $k_{13} = 1$, $k_{14} = 1$, $k_{15} = 1.5$, $k'_{16} = 1$, $k''_{16} = 3$, $V'_2 = 0.025$, $V''_2 = 1$, $V'''_2 = 1$, $V'_{12} = 0.2$, $V''_{12} = 100$, $V'''_{12} = 50$, $V_{17} = 0.93$, $V'_{17} = 0.2$, $V_{18} = 5$, $V'_{18} = 0.05$, $V_{19} = 0.25$, $V_{20} = 1$, $V_{21} = 1$, $V_{22} = 0.25$, $\gamma = 0.00462$

Michaelis and other constants (*for wild-type cells, dimensionless*)

$J_3 = 0.04$, $J_4 = 0.04$, $J_5 = 0.3$, $J_7 = 0.001$, $J_8 = 0.001$, $J_9 = 0.01$, $J_{10} = 0.01$, $J_{15} = 0.01$, $J_{16} = 0.01$, $J_{19} = 0.01$, $J_{20} = 0.01$, $J_{21} = 0.01$, $J_{22} = 0.01$, $k_D = 0.001$, $m_{NV} = 1$, $s_{NV} = 0.07$, $m_{DA} = 0.5$, $s_{DA} = 0.016$

We assume that the Tyr-15 phosphorylation state of Cdc2, i.e., the portion of Cdc2 phosphorylated, is the same in the Cdc13/Cdc2 dimer and in the Cdc13/Cdc2/Rum1 trimer. Therefore the concentration of MPF can be expressed as a simple ratio if $Cdc13_T$, *preMPF* and *Trimer* are known. TF, Wee1 and Cdc25 are considered to be zero-order ultrasensitive switches [42], existing in active and inactive forms. The sum of the concentration of the two forms is 1, meanwhile *TF*, *Wee1* and *Cdc25* mean the concentration of the active forms. The transitions between the two forms are enzyme-catalyzed reactions following Michaelis–Menten kinetics with parameters V_a, V_i, J_a and J_i (index a in subscript means activation, meanwhile index i means inactivation). Because the reactions in both directions are fast, instead of writing differential equations (as in the cases of *Ste9* or *IE*), we can write simple equations on their steady-state solutions. This is called the Goldbeter–Koshland function [42], indicated generally as $G(V_a, V_i, J_a, J_i)$, and the exact mathematical formula is given in [21].

[a] Italicized protein names (e.g. *Cdc25*) refer to the concentration of protein which is a dimensionless number. $Cdc13_T$, the total concentration of Cdc13/Cdc2 dimers (free *Cdc13* is assumed to be 0), including four different forms (Cdc2 in the complex can be phosphorylated at Tyr-15 or not, moreover both forms of the dimer can be bound to Rum1 or not); *preMPF*, the concentration of Cdc13/Cdc2 dimers having an inactivating phosphate group at Tyr-15, including two different forms (Rum1 either binds to the dimer or not); $Slp1_T$, the total concentration of Slp1, the sum of active and inactive forms; *Slp1*, the concentration of active Slp1; $Rum1_T$, the total concentration of free Rum1 and Rum1 bound to Cdc13/Cdc2, including two different forms (Cdc2 can be either phosphorylated at Tyr-15 or not); *Cig2*, the concentration of Cig2/Cdc2 dimers.

[b] Rum1 is assumed to bind quickly to Cdc13/Cdc2, independently of the Tyr-15 phosphorylation state of Cdc2 (for simplicity, the blocking effect of Rum1 on MPF is shown simply by a dashed line in Fig. 1). As a consequence, free Rum1 is present at a low level, and the concentration of Trimer (Cdc13/Cdc2/Rum1, where Cdc2 can be phosphorylated at Tyr-15 or not) can be expressed from a second order polynomial equation consisting of the dissociation constant of Trimer (k_D). *BB* is an auxiliary variable in this equation.

sequently, Cdc13 can accumulate, and Cdc13/Cdc2 together with Cig2/Cdc2 drives the cell into S phase. However, at first, most of the Cdc13/Cdc2 dimers are tyrosine-phosphorylated by Wee1. (The less active, tyrosine-phosphorylated form of Cdc13/Cdc2 is generally called preMPF.) Because there is an equilibrium distribution between preMPF and active MPF, and because the cell is growing in size, an increasing amount of active MPF accumulates in the nucleus. As its nuclear concentration increases, MPF is increasingly more effective at inactivating Wee1 and activating Cdc25. Hence, when the cell attains a sufficient size (i.e. a sufficient concentration of nuclear MPF), the positive feedback loops turn on and MPF gets fully activated, driving the cell into the M phase. Approximately 10 min later, MPF activates Slp1, which initiates the degradation of Cdc13, causing the cell to exit mitosis and reset back to G1 phase.

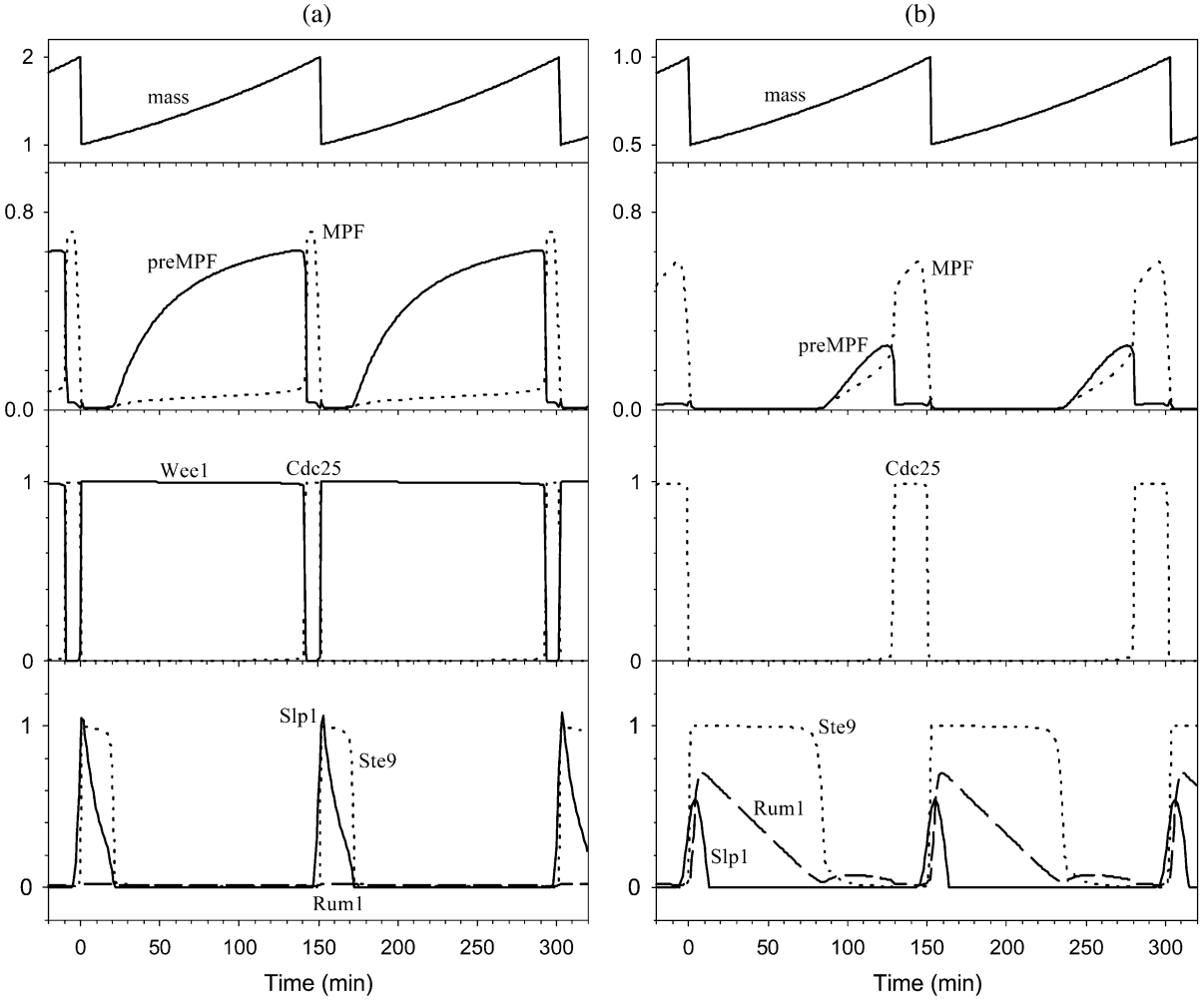

Fig. 2. Numerical simulations of cell cycles with the deterministic model (no stochastic effects). MPF refers to the concentration of active Cdc13/Cdc2 dimers. (a) Wild-type cells. Observe that Rum1 does not come up at mitotic exit, and Ste9/APC by itself cannot stabilize G1, therefore this phase is very short. (b) Mutant *wee1*$^-$ cells. In the absence of Wee1 (the principal tyrosine kinase that inhibits Cdc2), the cell executes mitosis at around half the size of WT cells. After mitosis, Rum1 comes up and, together with Ste9/APC, stabilizes G1 phase.

To simulate an average cell of a *wee1*$^-$ culture, we set the turnover number of the active form of Wee1 (V_{17}) to 0 (Fig. 2b). This mutant is half the size of WT cells, it has a long G1 phase (~ 80 min) during which Rum1 is stabilized, and a short G2 phase [44]. G2 is short because, in the absence of Wee1, Cdc25 phosphatase overwhelms the weak effect of the other Tyr-kinase (Mik1), whose activity (V'_{17}) we consider to be constant (for simplicity). Fig. 2a,b demonstrates that the deterministic model describes correctly the average properties of the two most important fission yeast cultures, WT and *wee1*$^-$.

2.2. Division asymmetry as a stochastic variable

Cell division in fission yeast, just like in other cell types, is not perfectly symmetrical, i.e. the sizes of the two newborn progenies may be slightly different. Since cell size at birth (*BL*, for birth length) has an influence on cycle time (*CT*), as we shall see, the stochastic variation in birth size makes the *CT* of the two sisters different [12]. Division asymmetry (*DA*) can be characterized by the distribution of a random variable, $DA = BL/DL$, where *DL* is the division length of the mother cell [14,45]. For a WT culture, *DA* is normally distributed with mean $\mu = 0.5$ and standard deviation (S.D.) $\sigma = 0.016$ [14]. Hence, to introduce division asymmetry into the simulation process, we compute a cell's birth size from its mother's division size by the formula $BL = DA \cdot DL$, where, at each division, *DA* is a new random number chosen from a normal distribution with $\mu = 0.5$ and $\sigma = 0.016$. By following the cells generation after generation, we simulate a population of asymmetrically dividing cells. (At a later stage, we will let nuclear volume vary as well.) We do not follow the cell cycle of the 'other' sister, with $BL = (1 - DA) \cdot DL$, but we will show later how to account for the correlated behavior of sister cells.

Numerical simulations of WT cells are summarized in Table 2. Asymmetric division generates some scattering in both *BL* and *CT*, but their coefficients of variation ($CV = \sigma/\mu$) are only half of the experimental values [14]. The *CV*s are small because a strong size control operates in G2 phase of the fission yeast cell cycle. As a consequence, all cells divide at much the same size, independently of birth length. Plotting *CT* as a function of *BL* (Fig. 3) gives the expected negative correlation, but the relationship is absolutely deterministic (no scatter), in contrast to experimental observations [14,46,47].

Table 2
Simulation results for WT and *wee1*$^-$ cultures, assuming asymmetric division ($CV_{DA} \neq 0$), but constant nuclear volume ($CV_{NV} = 0$)

Strain	WT	*wee1*$^-$
1. No. of cycles generated	245	245
2. *DA*	0.5 ± 0.016	0.5 ± 0.03
3. *CT* (min)	150.3 ± 6.33 (0.0421)	150.8 ± 13.33 (0.0884)
4. *BL* (relative)	1.00 ± 0.033 (0.0329)	0.50 ± 0.031 (0.0613)
5. *DL* (relative)	2.00 ± 0.0076 (0.0038)	1.00 ± 0.0000 (0.0000)
6. CV_{CT}/CV_{DL}	11.1	∞
7. slope *CT*/*BL* (min)	−192	−436
8. slope *Ext*/*BL*	−0.77	−1.00
9. slope CT_{s2}/CT_{s1}	−0.97 (0.947)	−1.00 (0.999)
10. slope CT_d/CT_m	0.13 (0.017)	0.0096 (0.000)

In rows 2–5, data are given as mean ± S.D., meanwhile in rows 3–5 the coefficient of variation (*CV*) is also indicated in parentheses. In rows 7–10, the slope of the appropriate regression line is given, and in rows 9–10, R^2 is also indicated in parentheses.

Division asymmetry alone does not explain other statistical properties of fission yeast cultures. The correlation between mother and daughter *CT*s should be negative [48], but our simulated population shows a weak positive correlation (Table 2), because *CT* values are determined almost exclusively by *BL*. To compute the correlation between sister *CT*s in the simulation, we exploit the fact that the function *CT*(*BL*) in Fig. 3 is absolutely deterministic and linear ($R^2 = 0.999$). Hence, the *CT* of the other sister cell which was not followed by the simulations must be $CT[DL \cdot (1 - DA)]$. Applying this rule, we find a strong negative correlation between sister *CT*s (Table 2), in sharp contrast to the expected positive correlation [48]. Sister *CT*s are

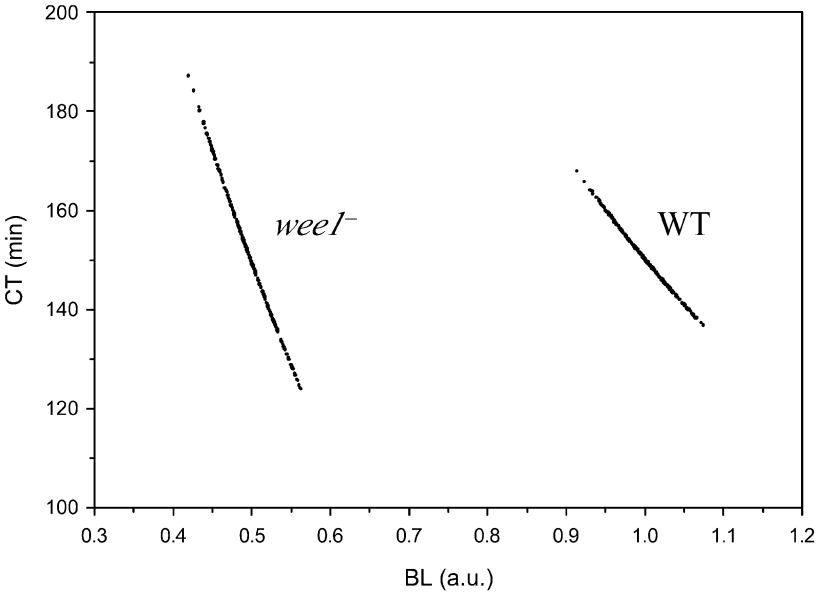

Fig. 3. Cycle time vs. birth length, simulated for a model containing asymmetric division as the only source of variability ($\mu_{DA} = 0.5$, $\sigma_{DA} = 0.016$ for WT cells, $\mu_{DA} = 0.5$, $\sigma_{DA} = 0.03$ for *wee1*$^-$ cells). The lack of scatter in these plots is grossly inconsistent with observations.

negatively correlated because the only source of stochasticity in this model is asymmetric division: if one of the sisters is larger than average, then the other must be smaller. The larger sister will have a smaller *CT*, while the smaller one has a larger *CT*.

A *wee1*$^-$ population was also simulated, assuming asymmetric division with a larger coefficient of variation ($CV_{DA} = 0.06$), as observed [14]. Although the larger variation in *DA* generates larger variations in *BL* and *CT* (Table 2), the computed *CV*s are still smaller than observed (note that the *CV*s in *wee1*$^-$ are twice as large as in WT [14]). We conclude that division asymmetry alone cannot account for observed variations in *CT* and *BL* in steady-state populations of WT and *wee1*$^-$ cells. Therefore, some other source of stochastic noise must contribute to cell cycle variability in fission yeast.

2.3. Nuclear volume as a second stochastic variable

Before introducing a second source of variability, we first discuss some assumptions of the model. Cell size ('mass' in Table 1) appears in the differential equations in two places: in the computation of MPF activity, and in the activation of TF by Puc1/Cdc2 and/or Pas1/Pef1 kinase. These assumptions are based on the idea that Cdc2/cyclin dimers accumulate in the nucleus, after being synthesized (step 1) in the cytoplasm. Because a larger cell has a larger capacity for protein synthesis, the number of Cdc2/cyclin dimers in the nucleus will be proportional to cell size. Since the effect of a Cdc2/cyclin complex most likely depends on its nuclear concentration (rather than the number of molecules in the nucleus), we introduce a new variable, nuclear volume (*NV*), and calculate nuclear concentration as (average cytoplasmic concentration)·(cell size)/(nuclear volume), as in Table 1. We assume that *NV* is a normally distributed random variable with $\mu = 1.0$ (arbitrary units) and a yet unknown σ. After mitosis, a new nucleus is formed whose volume is chosen from this normal distribution; thereafter, *NV* is kept constant until the next mitosis.

Because there is no experimental data on nu-

Table 3
Simulation results for WT and *wee1*$^-$ cultures, assuming asymmetric division ($CV_{DA} \neq 0$), and variable nuclear volume ($CV_{NV} \neq 0$)

Strain	WT	*wee1*$^-$
1. No. of cycles generated	244	244
2. *DA*	0.5 ± 0.016	0.5 ± 0.03
3. *NV*	1.0 ± 0.07	1.0 ± 0.10
4. *CT* (min)	150.7 ± 17.93 (0.119)	151.5 ± 32.29 (0.213)
5. *BL* (relative)	1.00 ± 0.064 (0.0637)	0.50 ± 0.054 (0.108)
6. *DL* (relative)	2.01 ± 0.115 (0.0571)	1.00 ± 0.094 (0.0934)
7. CV_{CT}/CV_{DL}	2.08	2.28
8. slope *CT*/*BL* (min)	−203	−467
9. slope *CT*/*NV* (min)	201	235
10. slope *CT*/*NCRB* (min)	189 (1.000)	106[a] (0.991)
11. slope *Ext*/*BL*	−0.88	−1.13
12. slope CT_{s2}/CT_{s1}	0.24 (0.044)	0.18 (0.027)
13. slope CT_d/CT_m	−0.38 (0.141)	−0.42 (0.173)
14. slope $\log_{10}\beta/t$ (h^{-1})	−2.25	−1.38

In rows 2–6, data are given as mean ± S.D., meanwhile in rows 4–6 the coefficient of variation (*CV*) is also indicated in parentheses. In rows 8–14, the slope of the appropriate regression line is given, and in rows 10, 12, 13, R^2 is also indicated in parentheses.

[a] Instead of a linear relationship, a second order polynom was used for calculating the missing sister's cycle time (see text).

clear volume in fission yeast, we treat σ_{NV} as an adjustable parameter, chosen to fit *CT* and *DL* distributions of the simulated population to experimental data [14]. For WT cells, a good fit is achieved with $\sigma_{NV} = 0.07$; see Table 3. Some consecutive cycles from the simulation are shown in Fig. 4a. Cycle time is negatively correlated with cell size at birth (Fig. 5a), and this graph is very similar to experimental observations [14,46]. Plotting $Ext = DL - BL$ vs. *BL* (Fig. 5b) gives a strong negative dependence (the slope of the regression line is not significantly different from −1), indicating that a strong size control operates in the cycle. Size control is called 'strong,' if any devia-

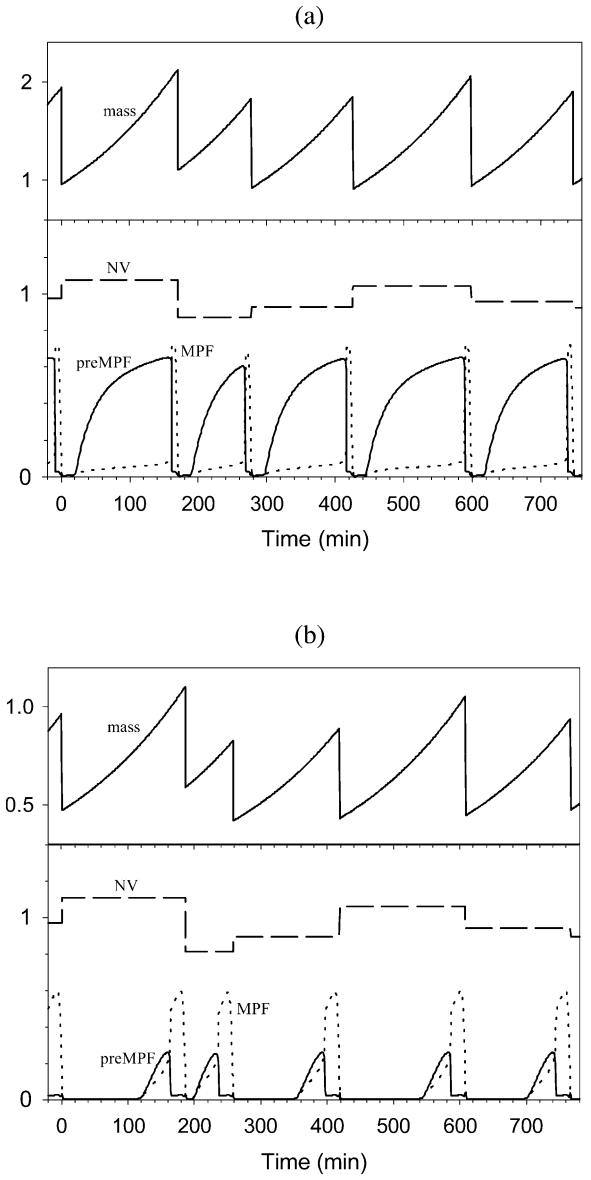

Fig. 4. Numerical simulations of cell cycles with two stochastic variables (division asymmetry and nuclear volume variability). (a) Wild-type cells ($\mu_{DA} = 0.5$, $\sigma_{DA} = 0.016$, $\mu_{NV} = 1.0$, $\sigma_{NV} = 0.07$). Observe that asymmetric division and changes in *NV* cause differences in both cycle time and birth size from one generation to the next. (b) Mutant *wee1*$^-$ cells ($\mu_{DA} = 0.5$, $\sigma_{DA} = 0.03$, $\mu_{NV} = 1.0$, $\sigma_{NV} = 0.1$). Larger variations in the stochastic parameters lead to larger variations in cycle time and birth size.

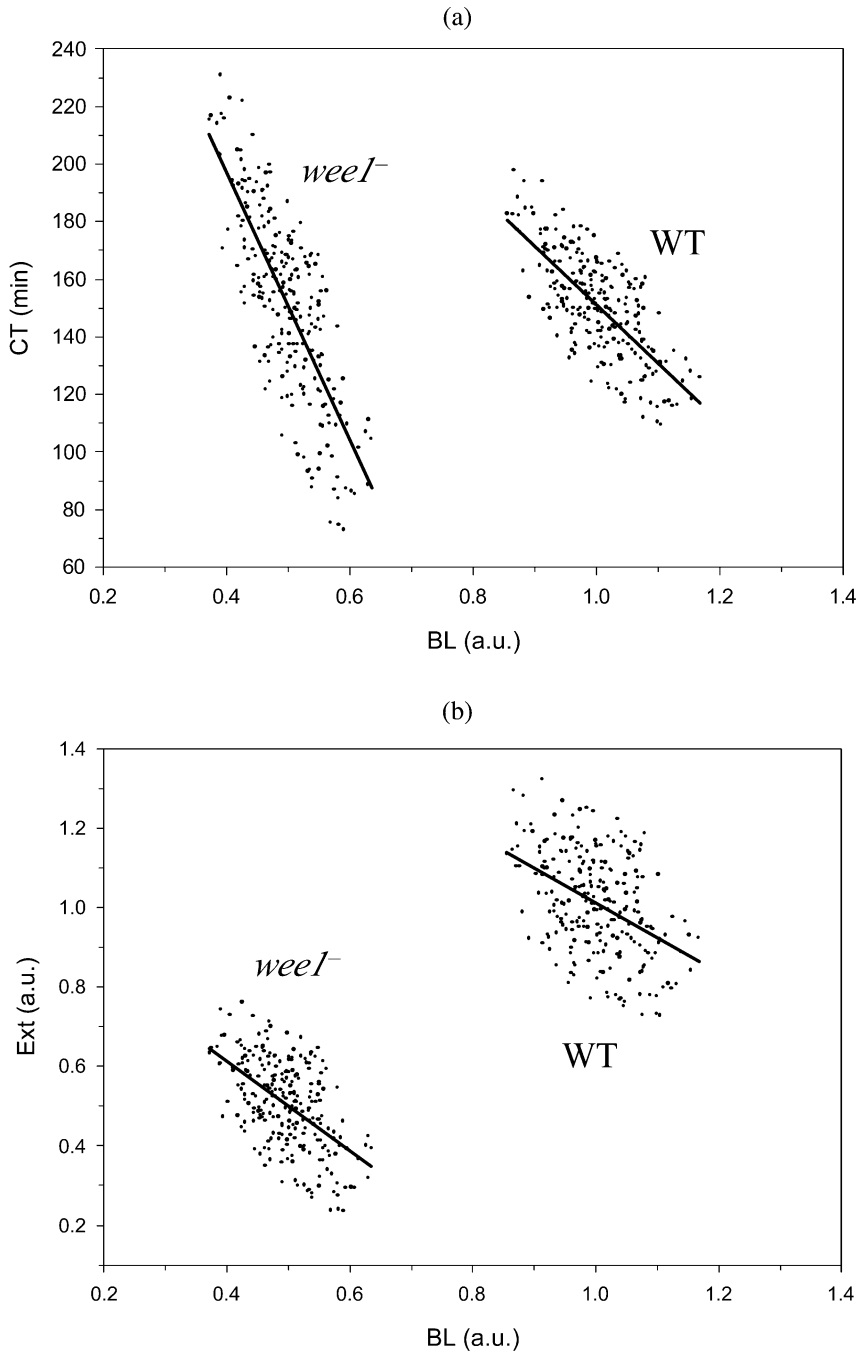

Fig. 5. (a) Cycle time vs. birth length, simulated for a model containing two stochastic variables (*DA* and *NV*). (b) Size extension vs. birth length in the same model. These plots compare favorably with experimental observations: Fig. 1 in [14].

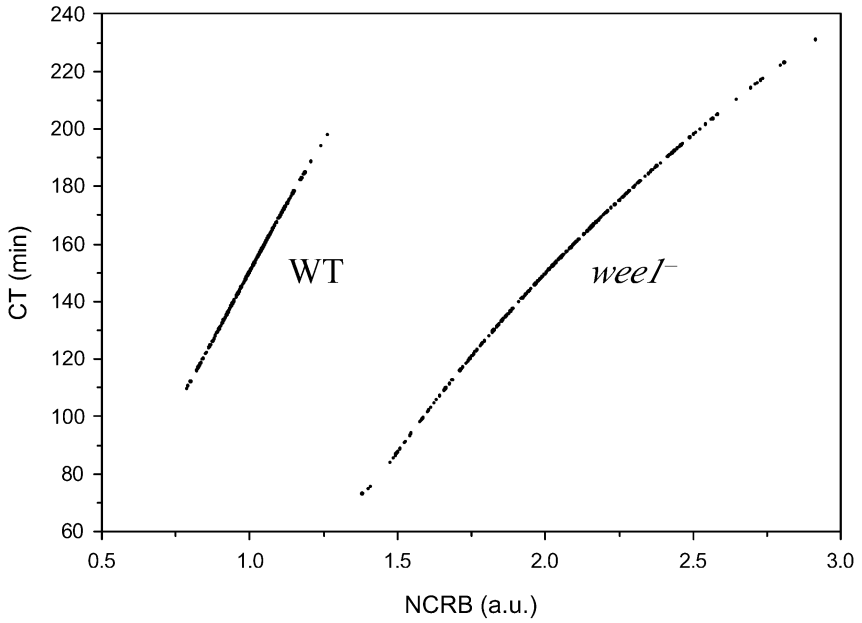

Fig. 6. Cycle time vs. nucleocytoplasmic ratio at birth, simulated for a model containing two stochastic variables (*DA* and *NV*).

tion from the average birth size is compensated within the subsequent cycle, as observed experimentally [14,46].

Let us define the nucleocytoplasmic ratio at birth as $NCRB = NV/BL$. Plotting CT vs. $NCRB$ (Fig. 6) gives a deterministic graph (no scatter), which is linear ($R^2 = 1.0$), at least for WT cells, implying that $NCRB$ rather than cell size determines inter-division time in this model.

This deterministic relation, $CT = CT(NCRB)$, can be used to calculate cycle time correlations of related cells (mother–daughter and sister–sister pairs). To calculate the CT of the 'other' sister cell (the one not followed in the simulation), we must generate a second, independent nuclear volume, call it NV_2, then calculate $NCRB_2 = NV_2/[DL \cdot (1 - DA)]$, and finally calculate the other sister's cycle time: $CT_2 = CT(NCRB_2)$. By this method, we computed correlations between CTs of mother–daughter and sister–sister pairs (Table 3), and found negative and positive correlations, respectively, in qualitative agreement with observations [48]. In quantitative terms, however, our simulated sister–sister correlation is too small and mother–daughter correlation is a bit large, in comparison with the experiment.

We have also compared our stochastic model to experimentally measured 'beta' curves [46,47] (Sveiczer, Novak and J.M. Mitchison, unpublished result). By definition [49], $\beta(t)$ is the probability that the absolute value of the difference in generation times for sister cells is greater than t. From our experimental data [14], we fit $\log_{10}\beta(t)$ vs. t to a straight line of slope $-2.38\ \mathrm{h}^{-1}$ (Sveiczer, Novak, J.M. Mitchison, unpublished result). For the simulated population (Table 3), the slope of the $\log_{10}\beta(t)$ vs. t is $-2.25\ \mathrm{h}^{-1}$, in excellent agreement with the experiment.

In order to fit the experimental data for a *wee1*$^-$ culture, we had to choose $\sigma_{NV} = 0.1$ (compared to the WT value of 0.07, see above). This is no surprise, considering that σ_{DA} is also larger for *wee1*$^-$ cells (0.03) than for WT cells (0.016). The general properties of a simulated *wee1*$^-$ culture are given in Table 3. Some representative cell cycles (Fig. 4b) are consistent with observations of cell cycle phases and temporal patterns of cell cycle regulators in *wee1*$^-$ mutants. Plots of

CT vs. *BL* and *Ext* vs. *BL* (Fig. 5a,b) are also consistent with experimental data [14]. For *wee1*$^-$ cells, the *CT* vs. *NCRB* graph (Fig. 6) is deterministic but non-linear. Using a second-order polynomial regression to fit the *CT* vs. *NCRB* relation, we have calculated, as before, the cycle times of related cells (Table 3). A β-curve was derived from our experimental data [14]. The slope of the regression line for $\log_{10}\beta$ vs. t is $-1.29\ h^{-1}$ (Sveiczer, Novak and J.M. Mitchison, unpublished result); and the simulations gave a similar result (Table 3).

3. Discussion

3.1. Parameter dependence of size controls

One of the fundamental mechanisms working during the cell cycle is size control, which ensures that the average size of cells in a steady-state population does not change during consecutive generations [50]. As early as the 1960s, size control was studied physiologically in many different organisms from bacteria to mammalian cells [46,51–53]. In eukaryotes, size control was found to act in G1 or in G2, delaying the onset of DNA replication or mitosis, respectively, until a critical cell size has been reached. The most extensive studies of size control were made with fission yeast, demonstrating conclusively that size control operates in G2 in WT cells and in G1 in *wee1*$^-$ cells [46,54]. The study of size control was somewhat neglected for the next 15 years, but in the last 5 years, attention has been paid again to this point [14,39,55,56] because of the wealth of new biochemical and genetic information on cell cycle regulation.

Indicators of strong size control are a characteristic ratio of CV_{CT} to CV_{DL} [11], and the regression slopes of plots of *Ext* vs. *BL* and *CT* vs. *BL* [13,14,46]. The present model fulfills the general requirements that CV_{CT}/CV_{DL} is ~ 2, and that strong negative correlations exist between *Ext* and *BL*, and between *CT* and *BL*. In the case of strong size control, the regression slope of *Ext* vs. *BL* should be close to -1, as observed experimentally in both WT and *wee1*$^-$ [14].

It is interesting to ask which parameters of the model (Table 1) are crucial in ensuring strong size control. To obtain strong mitotic size control in WT cells, the rates of synthesis (k_1) and degradation (V_2') of Cdc13/Cdc2 should be large, because, if the Cdc13/Cdc2 dimer is a relatively 'fast' variable (steps 1 and 2 are fast reactions), then mitosis starts at the same size irrespective of the cell's birth size. By decreasing these parameters, Cdc13/Cdc2 becomes a 'slow' variable, and the size control becomes weaker. The values we use ($k_1 = V_2' = 0.025\ min^{-1}$) are large enough to create a strong size control in G2. The slope (-0.88) of *Ext* vs. *BL* in our simulations is consistent with experiments [14,46].

To achieve a strong size control in G1 phase of small *wee1*$^-$ cells is more difficult. The length of G1 phase must be strongly dependent on birth size for cells significantly smaller than WT, but G1 duration must be short and nearly constant for cells close to WT size. To achieve this, Ste9 and Rum1 must be 'fast' variables, so as to create a stable G1 steady-state in *wee1*$^-$ cells, but this steady state must be missing in larger WT cells. Our parameter values satisfy these requirements.

3.2. The role of nucleocytoplasmic ratio in cell cycle regulation

It has been known for many decades that cell cycle times are correlated to the nucleocytoplasmic ratio in many different organisms [57–62]. This correlation has been understood in terms of some cytoplasmic molecule that must accumulate in the nucleus to drive certain cell cycle transitions (like G2/M), but the nucleus exerts an 'inhibitory' effect. One venerable possibility [63] is that the nucleus contains some titration sites along the chromosomes (whose quantity is, therefore, proportional to genome size), and these sites neutralize the incoming activator. Formerly published stochastic models of the fission yeast cell cycle [11–13] were based on this nuclear sites titration model [64], not taking into account the actual molecular circuitry of cell cycle regulation.

During the last decade, this circuitry has become more or less clear, making possible the development of realistic kinetic models of cell cycle progression in a variety of organisms, including fission yeast [24,65]. To date, these kinetic models have basically been deterministic (sets of non-linear ODEs). In this paper we try, for the first time, to combine a realistic model of cell cycle regulation with reasonable sources of stochasticity, in order to account for the observed variability in fission yeast cultures.

We have shown that asymmetric cell division alone is insufficient to explain all the statistical characteristics of fission yeast populations. For a second stochastic variable, we have chosen nuclear volume (NV), because we believe it is not the *quantity* of activator (Cdc2/cyclin) in the nucleus but rather its nuclear *concentration* that promotes cell cycle transitions.

In the present model, cycle time is perfectly determined by the nucleocytoplasmic ratio at birth, $NCRB = NV/BL$. (Note that the numerator in this definition is nuclear volume rather than genome size.) The perfect correlation between CT and $NCRB$ stems from three assumptions in the model: (1) NV is constant between divisions; (2) cell size is an exponential function of time; and (3) the G2/M transition is controlled by a strong size requirement. Certainly, none of these assumptions are perfectly satisfied, but we propose that the uneven distributions of birth sizes and nuclear volumes of sister cells are the major contributors to cell cycle variability. Other sources of variability, such as fluctuations in growth rate or random birth-and-death processes at the molecular level, we suspect to be considerably less important.

Acknowledgements

We are grateful to Dr Attila Csikasz-Nagy and Bela Gyorffy for helpful discussions. Our research was supported by the Howard Hughes Medical Institute (75195-542501), the Hungarian Scientific Research Fund (OTKA F-034100 and T-032015) and the USA National Science Foundation (DBI-9724085 and MCB-0078920). A. Sveiczer is grateful to the Hungarian Higher Education and Research Foundation for a Zoltan Magyary Postdoctoral Fellowship.

References

[1] B. Alberts, D. Bray, J. Lewis, M. Raff, K. Roberts, J.D. Watson, Molecular Biology of the Cell. 3rd ed., Garland Publishing, Inc, New York, 1994.
[2] P. Nurse, A long twentieth century of the cell cycle and beyond, Cell 100 (2000) 71–78.
[3] J.M. Mitchison, The fission yeast, *Schizosaccharomyces pombe*, Bioessays 12 (1990) 189–191.
[4] P. Nurse, Universal control mechanism regulating onset of M-phase, Nature 344 (1990) 503–508.
[5] P. Fantes, W. Grant, R. Pritchard, P. Sudbery, A. Wheals, The regulation of cell size and the control of mitosis, J. Theor. Biol. 50 (1975) 213–244.
[6] J. Tyson, W. Sachsenmaier, Is nuclear division in *Physarum* controlled by a continuous limit cycle oscillator? J. Theor. Biol. 73 (1978) 723–738.
[7] J. Smith, L. Martin, Do cells cycle? Proc. Natl. Acad. Sci. USA 70 (1973) 1263–1267.
[8] R. Brooks, D. Bennett, J. Smith, Mammalian cell cycles need two random transitions, Cell 19 (1980) 493–504.
[9] J. Tyson, K. Hannsgen, The distributions of cell size and generation time in a model of the cell cycle incorporating size control and random transitions, J. Theor. Biol. 113 (1985) 29–62.
[10] J.J. Tyson, O. Diekmann, Sloppy size control of the cell division cycle, J. Theor. Biol. 118 (1986) 405–426.
[11] W. Alt, J.J. Tyson, A stochastic model of cell division (with application to fission yeast), Math. Biosci. 84 (1987) 159–187.
[12] J.J. Tyson, Effects of asymmetric division on a stochastic model of the cell division cycle, Math. Biosci. 96 (1989) 165–184.
[13] A. Sveiczer, B. Novak, A stochastic model of the fission yeast cell cycle, ACH-Models Chem. 133 (1996) 299–311.
[14] A. Sveiczer, B. Novak, J.M. Mitchison, The size control of fission yeast revisited, J. Cell Sci. 109 (1996) 2947–2957.
[15] J.J. Tyson, Modeling the cell division cycle: cdc2 and cyclin interactions, Proc. Natl. Acad. Sci. USA 88 (1991) 7328–7332.
[16] A. Goldbeter, A minimal cascade model for the mitotic oscillator involving cyclin and cdc2 kinase, Proc. Natl. Acad. Sci. USA 88 (1991) 9107–9111.
[17] B. Novak, J.J. Tyson, Modeling the cell division cycle: M-phase trigger, oscillations and size control, J. Theor. Biol. 165 (1993) 101–134.
[18] B. Novak, J.J. Tyson, Numerical analysis of a comprehensive model of M-phase control in *Xenopus* oocyte extracts and intact embryos, J. Cell Sci. 106 (1993) 1153–1168.

[19] G. Marlovits, C.J. Tyson, B. Novak, J.J. Tyson, Modeling M-phase control in *Xenopus* oocyte extracts: the surveillance mechanism for unreplicated DNA, Biophys. Chem. 72 (1998) 169–184.

[20] A. Ciliberto, J. Tyson, Mathematical model for early development of the sea urchin embryo, Bull. Math. Biol. 62 (2000) 37–59.

[21] K.C. Chen, A. Csikasz-Nagy, B. Gyorffy, J. Val, B. Novak, J.J. Tyson, Kinetic analysis of a molecular model of the budding yeast cell cycle, Mol. Biol. Cell 11 (2000) 369–391.

[22] B. Novak, J.J. Tyson, Quantitative analysis of a molecular model of mitotic control in fission yeast, J. Theor. Biol. 173 (1995) 283–305.

[23] B. Novak, J.J. Tyson, Modeling the control of DNA replication in fission yeast, Proc. Natl. Acad. Sci. USA 94 (1997) 9147–9152.

[24] B. Novak, A. Csikasz-Nagy, B. Gyorffy, K. Chen, J.J. Tyson, Mathematical model of the fission yeast cell cycle with checkpoint controls at the G1/S, G2/M and metaphase/anaphase transitions, Biophys. Chem. 72 (1998) 185–200.

[25] J.J. Tyson, B. Novak, Cell Cycle Controls, in: C. Fall et al. (Eds.), Joel Keizer's computational cell biology, Springer-Verlag, Berlin–Heidelberg–New York, 2001. in press.

[26] B. Stern, P. Nurse, A quantitative model for the cdc2 control of S phase and mitosis in fission yeast, Trends Genet. 12 (1996) 345–350.

[27] M.A. Blanco, A. Sanchez-Diaz, J.M. de Prada, S. Moreno, $APC^{ste9/srw1}$ promotes degradation of mitotic cyclins in G_1 and is inhibited by cdc2 phosphorylation, EMBO J. 19 (2000) 3945–3955.

[28] S. Yamaguchi, H. Okayama, P. Nurse, Fission yeast Fizzy-related protein srw1p is a G_1-specific promoter of mitotic cyclin B degradation, EMBO J. 19 (2000) 3968–3977.

[29] J. Correa-Bordes, P. Nurse, $p25^{rum1}$ orders S phase and mitosis by acting as an inhibitor of the $p34^{cdc2}$ mitotic kinase, Cell 83 (1995) 1001–1009.

[30] K. Labib, S. Moreno, rum1: a CDK inhibitor regulating G1 progression in fission yeast, Trends Cell Biol. 6 (1996) 62–66.

[31] J. Benito, C. Martin-Castellanos, S. Moreno, Regulation of the G_1 phase of the cell cycle by periodic stabilization and degradation of the $p25^{rum1}$ CDK inhibitor, EMBO J. 17 (1998) 482–497.

[32] P. Russell, P. Nurse, Negative regulation of mitosis by *wee1*$^+$, a gene encoding a protein kinase homolog, Cell 49 (1987) 559–567.

[33] K. Lundgren, N. Walworth, R. Booher, M. Dembski, M. Kirschner, D. Beach, mik1 and wee1 cooperate in the inhibitory tyrosine phosphorylation of cdc2, Cell 64 (1991) 1111–1122.

[34] P. Russell, P. Nurse, *cdc25*$^+$ functions as an inducer in the mitotic control of fission yeast, Cell 45 (1986) 145–153.

[35] J.B.A. Millar, G. Lanaers, P. Russell, Pyp3 PTPase acts as a mitotic inducer in fission yeast, EMBO J. 11 (1992) 4933–4941.

[36] A. Murray, T. Hunt, The Cell Cycle. An Introduction, W.H. Freeman & Co, New York, 1993.

[37] T. Matsumoto, A fission yeast homolog of CDC20/p55CDC/Fizzy is required for recovery from DNA damage and genetically interacts with $p34^{cdc2}$, Mol. Cell. Biol. 17 (1997) 742–750.

[38] D. Fisher, P. Nurse, Cyclins of the fission yeast *Schizosaccharomyces pombe*, Semin. Cell Biol. 6 (1995) 73–78.

[39] C. Martin-Castellanos, M.A. Blanco, J.M. de Prada, S. Moreno, The puc1 cyclin regulates the G1 phase of the fission yeast cell cycle in response to cell size, Mol. Biol. Cell 11 (2000) 543–554.

[40] K. Tanaka, H. Okayama, A Pcl-like cyclin activates the Res2p–Cdc10p cell cycle 'start' transcriptional factor complex in fission yeast, Mol. Biol. Cell 11 (2000) 2845–2862.

[41] C. Martin-Castellanos, K. Labib, S. Moreno, B-type cyclins regulate G_1 progression in fission yeast in opposition to the $p25^{rum1}$ cdk inhibitor, EMBO J. 15 (1996) 839–849.

[42] A. Goldbeter, D.E. Koshland, Jr., An amplified sensitivity arising from covalent modification in biological systems, Proc. Natl. Acad. Sci. USA 78 (1981) 6840–6844.

[43] J.M. Mitchison, Cell Cycle Growth and Periodicities, in: A. Nasim, P. Young, B.F. Johnson (Eds.), Molecular Biology of the Fission Yeast, Academic Press, New York, 1989, pp. 205–242.

[44] P. Nurse, Genetic control of cell size at cell division in yeast, Nature 256 (1975) 547–551.

[45] E.O. Powell, A note on Koch and Schaechter's hypothesis about growth and fission of bacteria, J. Gen. Microbiol. 37 (1964) 231–249.

[46] P.A. Fantes, Control of cell size and cycle time in *Schizosaccharomyces pombe*, J. Cell Sci. 24 (1977) 51–67.

[47] H. Miyata, M. Miyata, M. Ito, The cell cycle in the fission yeast, *Schizosaccharomyces pombe*. I. Relationship between cell size and cycle time, Cell Struct. Funct. 3 (1978) 39–46.

[48] J.J. Tyson, The coordination of cell growth and division — intentional or incidental? Bioessays 2 (1985) 72–77.

[49] R. Brooks, D. Benneth, J. Smith, Mammalian cell cycles need two random transitions, Cell 19 (1980) 493–504.

[50] P.A. Fantes, P. Nurse, The cell cyclein: P.C.L. John (Ed.), Division Timing: Controls, Models and Mechanisms, Cambridge University Press, Cambridge, 1981, pp. 11–33.

[51] W.D. Donachie, Relationship between cell size and time of initiation of DNA replication, Nature 219 (1968) 1077–1079.

[52] J.R. Pringle, L.H. Hartwell, The molecular biology of the yeast *Saccharomyces*. Life cycle and inheritancein: J.N. Strathern, E.W. Jones, J.R. Broach (Eds.), The

Saccharomyces cerevisiae Cell Cycle, Cold Spring Harbor Laboratory, Cold Spring Harbor, 1982, pp. 97–142.
[53] D. Killander, A. Zetterberg, A quantitative cytochemical investigation of the relationship between cell mass and the initiation of DNA synthesis in mouse fibroblasts in vitro, Exp. Cell Res. 40 (1965) 12–20.
[54] P. Nurse, P. Thuriaux, Controls over the timing of DNA replication during the cell cycle of fission yeast, Exp. Cell Res. 107 (1977) 365–375.
[55] A. Sveiczer, B. Novak, J.M. Mitchison, Mitotic control in the absence of cdc25 mitotic inducer in fission yeast, J. Cell Sci. 112 (1999) 1085–1092.
[56] C.R. Carlson, B. Grallert, T. Stokke, E. Boye, Regulation of the start of DNA replication in *Schizosaccharomyces pombe*, J. Cell Sci. 112 (1999) 939–946.
[57] M. Hartmann, Über experimentelle Unsterblickheit von Protozoen-Individuen. Ersatz der Fortpflanzung von Amoeba Proteus durch fortgesetzte Regenerationen, Zool. Jahrb. 45 (1929) 973–987.
[58] D.M. Prescott, Relation between cell growth and cell division. III. Changes in nuclear volume and growth rate and prevention of cell division in *Amoeba proteus* resulting from cytoplasmic amputations, Exp. Cell Res. 11 (1956) 94–98.
[59] R.T. Johnson, P.N. Rao, Nucleo–cytoplasmic interactions in the achievement of nuclear synchrony in DNA synthesis and mitosis in multinucleate cells, Biol. Rev. 46 (1971) 97–155.
[60] J.J. Tyson, G. Garcia-Herdugo, W. Sachsenmaier, Control of nuclear division in *Physarum polycephalum*. Comparison of cycloheximide pulse treatment, UV irradiation, and heat shock, Exp. Cell Res. 119 (1979) 87–98.
[61] M. Dasso, J.W. Newport, Completion of DNA replication is monitored by a feedback system that controls the initiation of mitosis in vitro: studies in *Xenopus*, Cell 61 (1990) 811–823.
[62] P. Wang, S. Hayden, Y. Masui, Transition of the blastomere cell cycle from cell size-independent to size-dependent control at the midbastula stage in *Xenopus laevis*, J. Exp. Zool. 287 (2000) 128–144.
[63] W. Sachsenmaier, U. Remy, R. Plattner-Schobel, Initiation of synchronous mitosis in *Physarum polycephalum*. A model of the control of cell division in eukaryotes, Exp. Cell Res. 73 (1972) 41–48.
[64] J.J. Tyson, Size control of cell division, J. Theor. Biol. 126 (1987) 381–391.
[65] A. Sveiczer, A. Csikasz-Nagy, B. Gyorffy, J.J. Tyson, B. Novak, Modeling the fission yeast cell cycle: Quantized cycle times in *wee1*$^-$ *cdc25*Δ mutant cells, Proc. Natl. Acad. Sci. USA 97 (2000) 7865–7870.